

RESEARCH ARTICLE

10.1002/2015MS000434

Key Points:

- Cloud-radiative effects lead to a more realistic mean state and a better MJO
- In the convective MJO phase, the heating profile is more top-heavy
- Stronger Kelvin waves are connected with weaker MJOs

Correspondence to:

T. Crueger,
traute.crueger@mpimet.mpg.de

Citation:

Crueger, T., and B. Stevens (2015), The effect of atmospheric radiative heating by clouds on the Madden-Julian Oscillation, *J. Adv. Model. Earth Syst.*, 7, 854–864, doi:10.1002/2015MS000434.

Received 27 JAN 2015

Accepted 27 MAY 2015

Accepted article online 29 MAY 2015

Published online 16 JUN 2015

© 2015. The Authors.

This is an open access article under the terms of the Creative Commons Attribution-NonCommercial-NoDerivs License, which permits use and distribution in any medium, provided the original work is properly cited, the use is non-commercial and no modifications or adaptations are made.

The effect of atmospheric radiative heating by clouds on the Madden-Julian Oscillation

Traute Crueger¹ and Bjorn Stevens¹

¹The Atmosphere in the Earth System, Max Planck Institute for Meteorology, Hamburg, Germany

Abstract This article explores how atmospheric radiative heating, due to the presence of clouds, influences the Madden-Julian Oscillation (MJO) as simulated by four comprehensive atmosphere general circulation models. Simulations in which clouds are transparent to electromagnetic radiation (“clouds-off”) are compared with control simulations in which clouds are allowed to interact with radiation (“clouds-on”). Making clouds transparent to radiation leads to robust changes of the mean state: the westerly winds in the equatorial Indo-Pacific area weaken and the precipitation reveals a shift from single to double Intertropical Convergence Zones. These changes are accompanied by weaker MJOs. Also, the moisture sensitivity of precipitation changes, however not consistently within our group of models. Further analyses show that within the active phase of intraseasonal variability, cloud-radiative effects amplify the heating profiles compared to clouds-off. Heating from nonradiative processes is dominated by the parameterized convection, but large-scale heating associated with cloud microphysical processes acting on the grid-scale modifies the shape of the heating profile, leading to a top-heaviness when cloud-radiative effects are accounted for. The radiative heating due to clouds slows down the phase speed of the MJO. Averaged over the entire MJO life cycle, the column-integrated radiative heating due to clouds lags the vertically integrated moist static energy by 40°–60° of longitude (equivalently 7–10 days assuming a period of 60 days). All four models studied reveal more pronounced Kelvin waves when clouds are transparent to radiation, suggesting that cloud-radiative effects on large-scale heating profiles damp smaller scale, or faster, Kelvin waves and amplify MJO-like disturbances.

1. Introduction

The Madden-Julian Oscillation (MJO) represents the dominant mode of intraseasonal variability in the tropics. Comprehensive general circulation models (GCMs) poorly represent MJO-like variability, and improving the latter is difficult, because of a poor understanding of the processes involved in the MJO. Among the various processes associated with the MJO, the interaction between clouds and radiation has repeatedly been identified to be an important one. This interaction has been investigated theoretically and in GCM studies. Most studies suggest that cloud-radiative effects are important for the development and amplitude of the MJO. In a pioneering theoretical study, *Bony and Emanuel* [2005] demonstrated how cloud-radiative effects may amplify tropical intraseasonal variability. In particular, by reducing the phase speed of large-scale tropical disturbances, cloud-radiative effects imbue the disturbances with a character more recognizable as the MJO. *Sobel and Maloney* [2013] used a linear moisture-mode model to likewise show that cloud-radiative effects are necessary to destabilize an intraseasonal mode, which they interpret as their model’s MJO. In individual GCM studies, cloud-radiative effects have been eliminated or reduced [*Lee et al.*, 2001; *Andersen and Kuang*, 2012; *Kim et al.*, 2011b; *Lau et al.*, 2005; *Lin et al.*, 2007]. *Lin et al.* [2007] found that the MJO-like disturbances disappeared from a super-parameterized GCM when cloud-radiative effects were excluded. *Lin et al.* [2007] and *Lee et al.* [2001] found that cloud-radiative effects also influence Kelvin waves and their propagation speed. However, their control experiment as well as their experiment excluding cloud-radiative effects did not reveal MJO-like variability, and so they could not study the radiative effects of clouds on the MJO. In contrast to the aforementioned studies, *Lau et al.* [2005] found that the MJO simulated in their GCM strengthens and is more eastward propagating when cloud-radiative effects are reduced.

In this study, a small ensemble of GCM simulations is investigated to explore the extent to which cloud-radiative effects have a robust influence on the MJO, and on convectively coupled equatorial Kelvin waves.

To do so, we use the Clouds On/Off Climate Interaction Experiment (COOKIE) [Stevens *et al.*, 2012] protocol that was developed in the context of the European Union Cloud Intercomparison, Process Study & Evaluation Project, EUCLIPSE. COOKIE describes an experimental protocol in which the radiative properties of clouds were systematically altered to study the cloud-radiative effects on circulations. In this study, we use the clouds-off experiments, within which clouds were made transparent to all forms of electromagnetic radiation globally. These are compared to control simulations (within which clouds interact with radiation). In each case, 30 year simulations with prescribed sea-surface temperatures are performed, following the atmospheric model intercomparison project (AMIP) protocol [Gates, 1992] as prescribed in the fifth phase of the coupled model intercomparison project [Taylor *et al.*, 2012]. The COOKIES were performed with four different GCMs, but within an identical experiment framework, thus allowing for the identification of common responses to cloud-radiative interactions. The aim of this study is to use these simulations to enhance our understanding of how cloud-radiative interactions affect the MJO. The COOKIES have also been used to study radiative effects of low clouds on tropical precipitation [Fermepin and Bony, 2014], and the role of cloud-radiative effects on midlatitude circulations (Y. Li *et al.*, The influence of cloud radiative effects on the large-scale atmospheric circulation, submitted to *Journal of Climate*, 2014).

The present study focuses on the effect of the mean state of Indo-Pacific lower tropospheric winds and precipitation, the moisture sensitivity of rain rates, and the vertical structure of heating.

2. Models and Experiments

We investigate experiments conducted with four state of the art comprehensive general circulation models. The CNRM-CM5 which is developed by Météo-France [Voltaire *et al.*, 2013], the MRI-CGCM3 of the Meteorological Institute of Japan [Yukimoto *et al.*, 2012], the MPI-ESM developed by the Max Planck Institute for Meteorology in Hamburg Germany [Stevens *et al.*, 2013], and the IPSL-CM5 whose physical component is developed by the group at the Laboratoire de Météorologie Dynamique in Paris, France [Dufresne *et al.*, 2013]. The CNRM-CM5, MRI-CGCM3, and IPSL-CM5 experiments were performed with an identical version that has been used for the Coupled Model Intercomparison Project 5 (CMIP5) [Taylor *et al.*, 2012]. For ECHAM6, the atmospheric module of the MPI-ESM, a slightly newer version has been utilized, namely ECHAM6.1.05. But there is no evidence that ECHAM6.1.05 meaningfully differs from the version used to perform the CMIP5 experiments. The AMIP protocol is used to define the control experiments, so that for all the models except the MPI-ESM, the CMIP5 AMIP experiment serves as the control experiment, hereafter referred to as “clouds-on”. In the “clouds-off” experiments, clouds were made globally transparent to electromagnetic radiation by setting the cloud cover to zero in the call to radiation within the model. All experiments simulated a 30 year period, from 1979 to 2008, with prescribed monthly mean sea-surface temperature (SST) and sea ice concentration (SIC). The authors are aware that the experiment setup of COOKIE is not perfect, because the land temperatures are allowed to respond to the changes of the radiation code, while the SSTs are not. Actually, we find increased precipitation over the tropical land in clouds-off compared to clouds-on (see Figure 1), which we suggest result from increased land temperatures that in turn induce lower tropospheric advection of moist air from the oceans toward the land. Apart of that, the radiation manipulations primarily influence the atmospheric heating, and as such is dominated by long-wave cloud-radiative effects.

The authors evaluate daily output of precipitation, relative humidity (RH), and the zonal wind at 850 hPa (u_{850}) and 200 hPa (u_{200}) from all the models. For the MPI-ESM experiments, it was possible to perform additional diagnostics to help in the analysis of daily heating rates and the effect of cloud-radiative heating conditioned on the moist static energy budget. This more detailed analysis facilitates a comparison to the theoretical ideas developed in past studies, e.g., Bony and Emanuel [2005]. The intraseasonal signal is defined in terms of the 20–100 day band-pass-filtered values of a particular variable [Duchon, 1979].

3. Results

3.1. Mean State

The mean atmospheric state is believed to be important for the initiation of an MJO. Past work has demonstrated that both the zonal extent of the mean surface westerly winds across the Indo-Pacific region and the mean precipitation are relevant for a realistic MJO simulation [Slingo *et al.*, 1996; Sperber *et al.*, 2005;

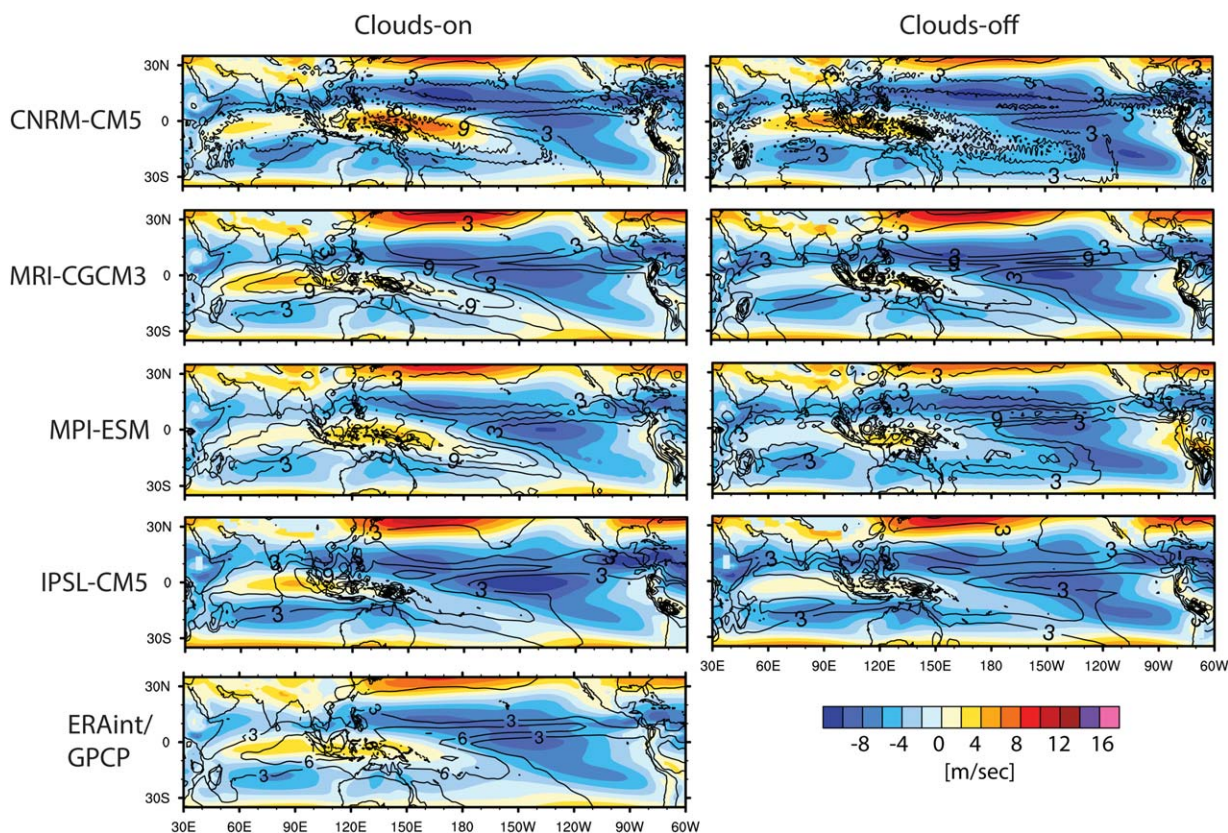


Figure 1. November–April mean precipitation (contour lines, increment: 3 mm/d), and 850 hPa zonal wind (m/s) (shaded) for (left) clouds-on and (right) clouds-off for the models and (bottom left) ERA-interim/GPCP. Period: 1979–2008, ERAint/GPCP: 1989–2008.

Zhang et al., 2006; Lin et al., 2007; Waliser et al., 2009; Kim et al., 2011a]. In addition, humidity, especially the feedback between moisture and convection had been found to be important with respect to the models’ skill to simulate a realistic MJO [Kim et al., 2014b; Thayer-Calder and Randall, 2009; Grabowski and Moncrieff, 2004]. In all models, our analysis reveals changes of these mean characteristics in response to switching-off cloud-radiative feedbacks.

Observations as well as simulations show that the MJO prefers low-level and surface mean westerlies across the Indo-Pacific warm pool area. If the zonal extension or the magnitude of the westerlies is too small, then the simulated MJOs are often too weak [e.g., Waliser et al., 2009; Zhang et al., 2006]. In clouds-on, all models show equatorial westerlies, which however deviate to a certain extent from the ERA-interim Reanalysis winds [Dee et al., 2011]. Either the model westerlies are too weak over the Indian Ocean (MPI-ESM and CNRM-CM5), or the eastern Pacific (MRI-CGCM3, IPSL-CM5), or they are too pronounced over the eastern Pacific (CNRM-CM5). This is apparent from Figure 1 showing the mean precipitation and 850 hPa wind fields, averaged over the main MJO season November–April [Waliser et al., 2009]. Overall, in all models, the westerlies weaken in response to switching off the cloud-radiative interaction. For MPI-ESM and MRI-CGCM3, only weak westerlies still appear in a small area over the Maritime Continent. In CNRM-CM5 clouds-off, the westerlies over the Indian Ocean get stronger, while over the west Pacific they nearly disappear. For IPSL-CM5, there is a general reduction of the wind speed of the westerlies in the Indo-Pacific area.

Most precipitation is reasonably well represented in the clouds-on experiments, however, with overall too high amounts (Figure 1). In all clouds-off experiments (except IPSL-CM5), we find an increase of precipitation (averaged from April to November) over the Maritime Continent and also over parts of South America compared to clouds-on (see section 2). In addition, the clouds-off experiments reveal a tendency toward a double Intertropical Convergence Zone (ITCZ). This is especially apparent across the Pacific Ocean but also occurs over the Indian Ocean, where the MJO initiates. The single ITCZ over the Indian Ocean is generally well represented in the clouds-on (standard AMIP) simulations by the MPI-ESM and MRI-CGCM3 models,

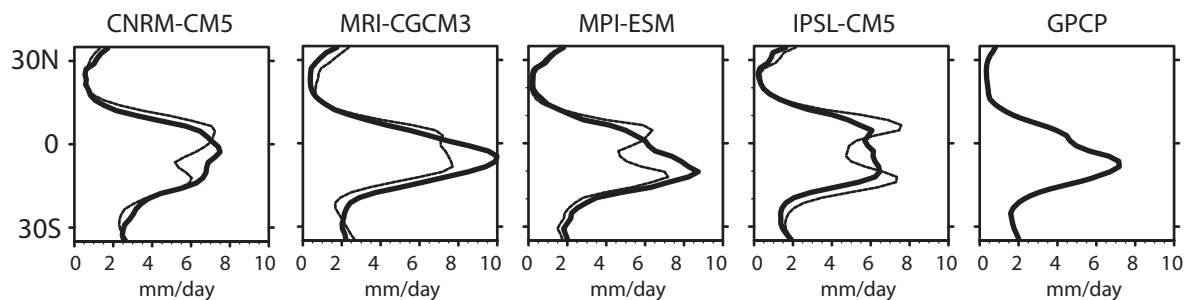


Figure 2. Latitudinal structure of precipitation rates averaged over 60°E–90°E and November–April for clouds-on (thick line) and clouds-off (thin line) (mm/d). Period: 1979–2008, for GPCP 1998–2007 [Huffman et al., 2001].

although the latter yields a too pronounced single maximum (Figure 2). In the clouds-on simulation by the CNRM-CM5 and IPSL-CM5 models, there is a less pronounced single ITCZ structure. However, all models show evidence of a double ITCZ in their clouds-off experiment, to a degree that is especially pronounced in the MPI-ESM and IPSL-CM5 simulations.

The relative humidity (RH) response to switching-off cloud-radiative feedbacks is not as consistent among the models as it is for precipitation and the wind fields. This is evident in Figure 3 showing the RH profiles binned by daily rain rates in the Indian Ocean area (15°S–10°N, 60°E–90°E). CNRM-CM5 clouds-on shows the largest similarities with the observational-based figure (top right of Figure 3), namely the minimum around 500 hPa for the lowest rain rates, and a roughly constant RH gradient with higher rain rates between 400 and 800 hPa (note the log-scale for the daily rain rates). However, the gradient is too large for small and too small for large (convective) rain rates, and the tropopause region is too dry. This is also the case for the other clouds-on experiments. These experiments additionally show deviations with respect to the observations, in that they are too dry below (MPI-ESM) or above (IPSL-CM5) 600 hPa or too wet for high rain rates smaller than 100 mm/d (MRI-CGCM3). The response to switching-off cloud-radiative feedbacks is different among the models: for high rain rates, CNRM-CM5 reveals a wetter atmosphere, i.e., there is no RH gradient for larger (convective) precipitation rates between 400 and 800 hPa. A drying is found in the midlower troposphere for MPI-ESM and to some extent in MRI-CGCM3, the latter sharing more similarities with the observations in clouds-off than in clouds-on. Overall, IPSL-CM5 clouds-off is dryer than clouds-on and reveals the smallest maximal rain rates.

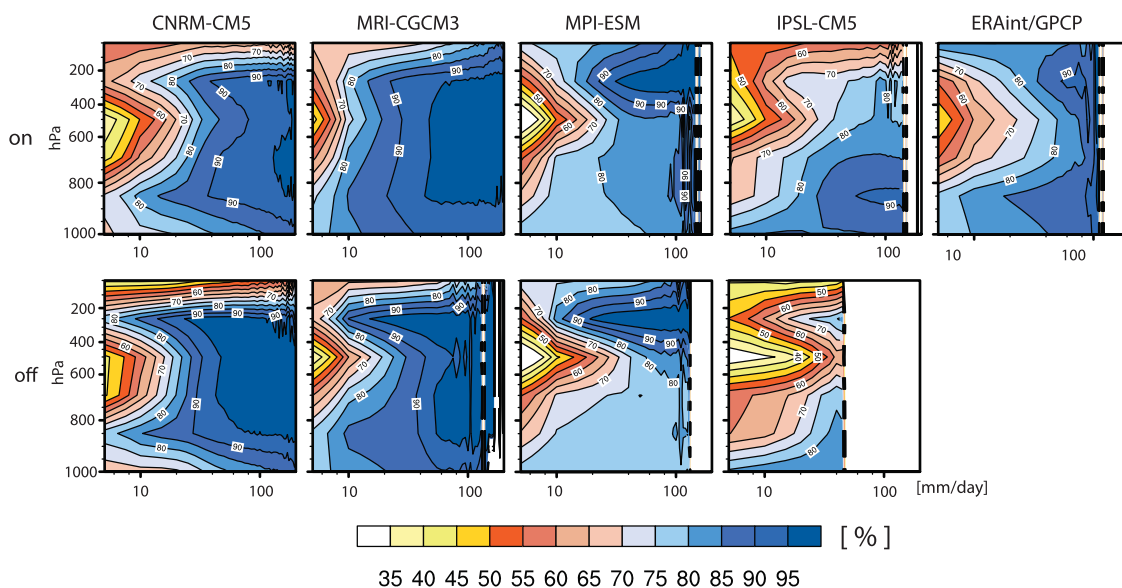


Figure 3. Composite profiles of relative humidity binned by daily average precipitation rates (mm/d) in the area 15°S–10°N, 60°E–90°E. (top) Clouds-on and (bottom) clouds-off; season: November–April; period: 1979–2008, for GPCP 1998–2007.

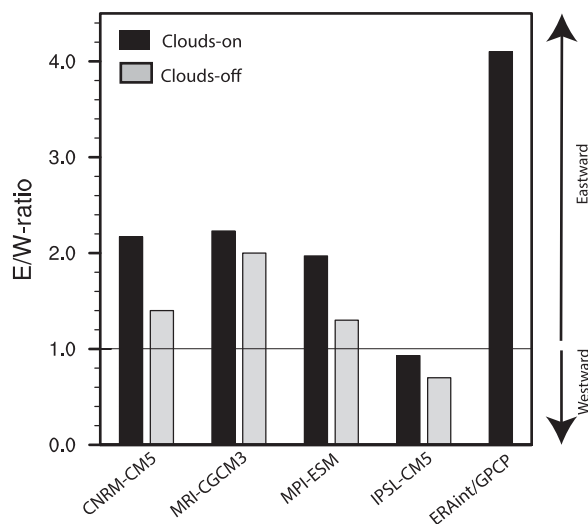


Figure 4. Ratios of eastward/westward propagation power within the MJO frequency wave number ranges (frequency: 1/20 to 1/100 1/d; wave numbers: 1–3). Mean ratios for equatorial precipitation, u_{850} and u_{200} (1979–2008). Also included is the mean ratio for ERA-interim winds and GPCP precipitation (1998–2007) [Huffman et al., 2001; Dee et al., 2011] (season: November–April).

ratio of the power in eastward versus westward moving features within the MJO wave number/frequency ranges, which [following Waliser et al., 2009] we choose as the wave numbers 1–3 and frequencies 100^{-1} to 20^{-1} d^{-1} . In constructing Figure 4, we average the ratios in precipitation and zonal winds (u_{850} and u_{200}) for the November–April period, which represents the main MJO season. Past work has demonstrated that this is a useful indicator of the overall eastward propagation strength of the MJO [Crueger et al., 2013]. A ratio larger than one indicates an eastward propagating disturbance, a ratio smaller than one is indicative of more power in a westward propagating disturbance. All models, except IPSL-CM5, produce simulations with more power in the eastward propagating signal in clouds-on, albeit the eastward dominance is clearly less pronounced than what is found in the reanalysis of meteorological data (ERA-interim Reanalysis) [Dee et al., 2011]. With clouds being transparent to radiation, all models produce simulations with reduced eastward/westward ratios as compared to the control experiment (clouds-on). The reduction is especially clear for MPI-ESM and CNRM-CM5. Because the IPSL-CM5 model does not exhibit more power in eastward propagating (versus westward propagating) signals in the control simulation, it is something of an outlier. Even so, when cloud-radiative effects are removed, the eastward propagation becomes relatively smaller, consistent with the simulations by the other models.

The MJO is often discussed in the context of convectively coupled equatorial waves (CCEWs). Kim et al. [2011b] found for the Seoul National University GCM a dependency between the MJO and the Kelvin waves, in that when the MJO gets stronger, the Kelvin waves weaken. Therefore, we explore, whether this dependency is also found for our group of models. To do so, we calculate the wave number-frequency spectra of precipitation. The MJO and the Kelvin waves appear in the symmetric part of the spectrum [Kiladis et al., 2009], which is shown in Figure 5. The spectra suggest that cloud-radiative heating influences both the MJO and the Kelvin waves. In experiments, in which cloud-radiative effects are disabled, the Kelvin waves are much stronger and the MJO signal is generally weaker (see also Figure 4). Therefore, the present analysis suggests a common sensitivity of Kelvin waves and the MJO to cloud-radiative interactions. It is not clear, if this link merely reflects a differential response to cloud-radiative effects, or if the suppression of one feature enhances the other.

3.3. Atmospheric Heating Rates

Making clouds transparent to radiation directly affects atmospheric heating rates. Radiative heating in the atmosphere is a source of moist static energy (MSE), which in turn is tightly related to deep convection [Neelin and Held, 1987; Bony and Emanuel, 2005; Maloney, 2009; Chikira, 2013]. Because the focus of this

Thus, eliminating cloud-radiative feedbacks generally tends to modify the mean state of precipitation and the lower tropospheric winds in a way that is—according to the literature—related to a weaker MJO. Actually—this will be shown in the next section—the MJO shows a robust and consistent change in response to switching-off cloud-radiative feedbacks within the group of four models studied here. The changes of humidity do not show such a consistent picture but the relationship between humidity and convection is also known to be very model dependent.

3.2. MJO and Kelvin Waves

Consistent changes in response to making clouds transparent to radiation (clouds-off) occur for the MJO simulated by the models. This is illustrated in Figure 4 by the amount of variance in eastward propagating signals within the equatorial belt (10°S – 10°N). The eastward propagation is measured by the

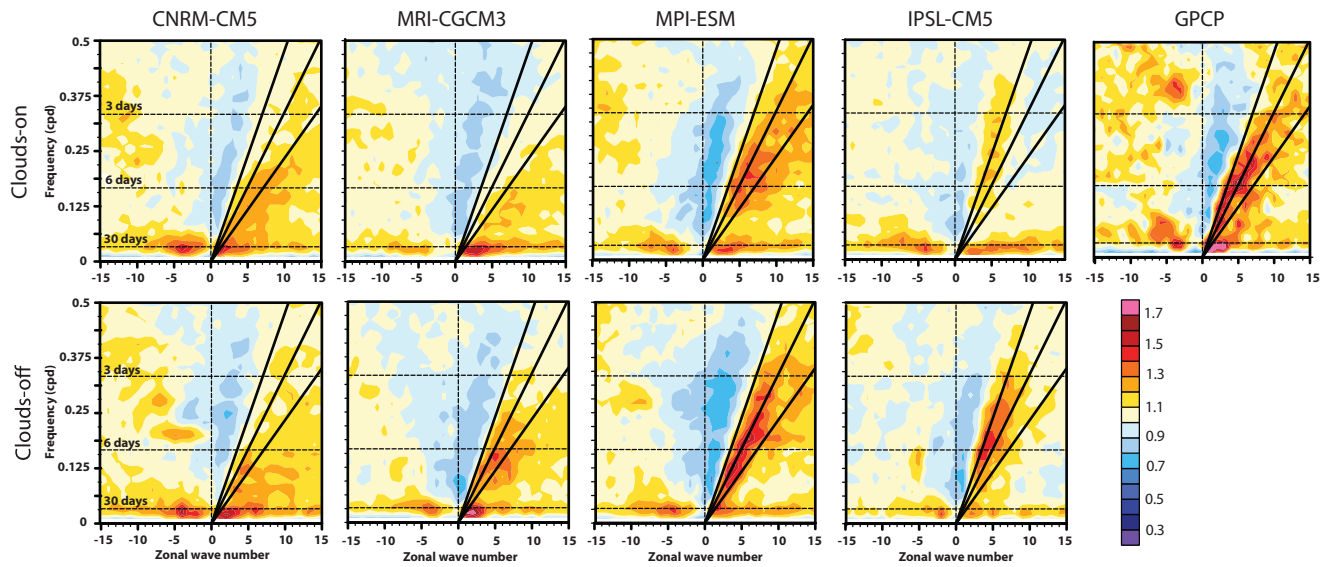


Figure 5. Wave number-frequency power spectra of the symmetric component of precipitation, summed from 13°N to 13°S, plotted as ratios between raw power and the power of smoothed red noise background spectra. Positive/negative wave numbers represent eastward/westward propagating waves. Dispersion curves are shown for Kelvin waves for equivalent depths of 12, 25, and 50 m. The MJO signal appears on the eastward propagating part with wave numbers 1–3 and periods longer than 30 days. (top) Clouds-on and (bottom) clouds-off. Period: 1979–2008, for GPCP: 1998–2007 [Kiladis et al., 2009].

study is on cloud radiation effects, our analysis focuses on the longwave (LW) heating of clouds. Changes in the shortwave heating of the surface are important over land (where surface temperatures are not prescribed), but because clouds are nearly perfect scatterers, plays less of a role in the atmosphere (see e.g., Li, submitted manuscript, 2014).

To understand how cloud-radiative heating influences the MJO, we composite vertically integrated heating rates and moist static energy on an MJO index (Figure 6). The MJO index ($M(t)$) is calculated from

$$M(t) = PC_1(t)^2 + PC_2(t)^2, \tag{1}$$

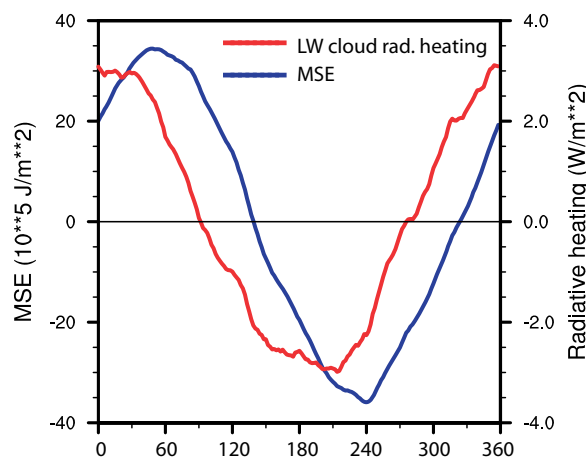


Figure 6. MJO composites of equatorial vertically integrated MSE (blue) (J/m^2), and longwave cloud-radiative heating anomalies (red) (W/m^2) for MPI-ESM clouds-on. First, composites were established with respect to $M(t) > 1$ for all MJO life cycle phases (here: 192). Then, these 192 composites were averaged. Before averaging, the single composites were zonally shifted according to their individual phase shift with respect to a reference composite. (November–April, 20–100 day filtered, x axis: arbitrary longitude).

where $PC_i(t)$ represents the i th principal component of the multivariate Empirical Orthogonal Function (EOF) based on 20–100 day filtered and normalized precipitation, u_{850} and u_{200} , averaged from 15°S to 15°N. $M(t)$ is calculated following Wheeler and Hendon [2004] and Waliser et al. [2009], except that we utilize precipitation instead of outgoing longwave radiation. This has been done to avoid biased results due to the manipulation in the radiation code and because the link between OLR and precipitation may be biased in the model. The compositing threshold of the MJO index is defined to be larger than one, and the phases of the MJO life cycle are obtained from the phase relationship between $PC_1(t)$ and $PC_2(t)$. Overall, 192 life cycle phase composites were created (one for each of the grid points around a latitude circle in MPI-ESM), thus between two composites there is a zonal shift of 1.875°. Shifting each

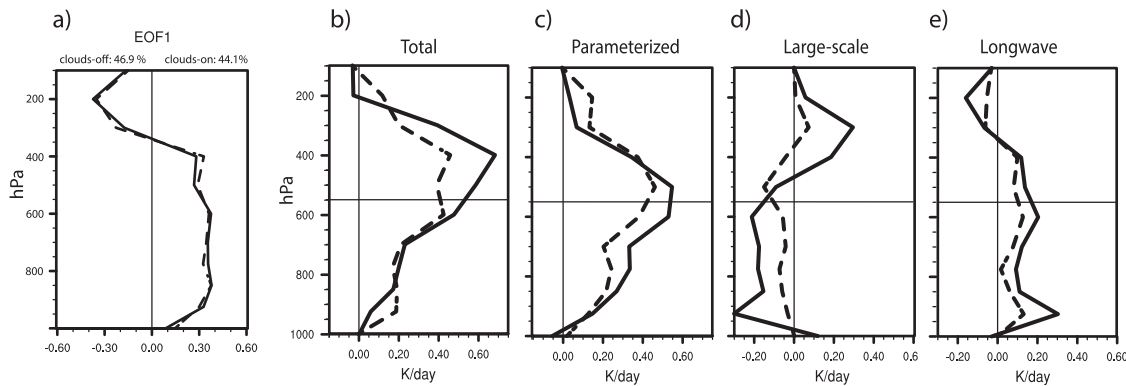


Figure 7. (a) EOF₁ of intraseasonal LW radiative heating averaged over 15°S–10°N and 60°E–90°E for MPI-ESM. (b–e) Heating rates regressed to the PC of EOF₁. (b) Total heating, (c) parameterized, (d) large scale, and (e) longwave. Thin black horizontal line roughly represents the freezing level (solid: clouds-on; dashed: clouds-off).

single composite according to its total shift with respect to a reference composite and then averaging over all composites leads to Figure 6.

The curves in Figure 6 reveal a wave number one oscillation for both the LW cloud-radiative heating and the MSE. The heating lags the MSE anomaly by 40°–60°, i.e., 7–10 days (assuming a period of 60 days). Hence, the radiative effects of clouds act to increase MSE on the westward flank of the MJO, thereby slowing it down. Similar results are obtained when including SW cloud-radiative heating, as shortwave atmospheric heating rates are, as expected, small (not shown).

3.4. Vertical Profiles of Heating

Clouds exert a considerable effect on the heating rates. Thus, making clouds transparent to radiation is expected to change the vertical structure of heating [e.g., Houze, 1982]. In the literature, it is often discussed, whether and how the shape of the total heating profile and its components vary with the MJO [e.g., Lappen and Schumacher, 2012; Li et al., 2009]. To contribute to this discussion, we perform a regression analysis of the single heating components based on the convective heating profile that is associated with intraseasonal variability. The procedure roughly follows that of Mehta and Smith [1997], who conducted an EOF analysis to establish the LW heating profile that represents deep convection. The EOF time series is afterward utilized to perform a regression analysis of the (unfiltered) condensational heating rates. We average over the MJO initiation area and filter intraseasonally (20–100 day filter), because we search for intraseasonal deep convection, especially in that region. We decompose

$$Q_{LW}(p, t) = \sum_{N=1}^n E_n(p) * P_n(t) \quad (2)$$

where $E_n(p)$ is the basis of the n th EOF and represents vertical structures of LW heating, while $P_n(t)$ is the corresponding anomaly time series (principal component) and describes the temporal variability of $E_n(p)$ [von Storch and Zwiers, 1999]. The leading EOF, $E_1(p)$ is characterized by a profile with one zero crossing at about 350 hPa with warming below and cooling above (Figure 7a). According to Mehta and Smith [1997], a similar LW heating profile accompanies convectively active phases. Therefore, the corresponding time series can be used for the regression procedure.

$E_1(p)$ reveal similar shapes for clouds-on and clouds-off (Figure 7a) and differ mainly with respect to the variances they explain (46.9% in clouds-off and 44.1% in clouds-on). The regression analysis for MPI-ESM clouds-on leads to a total heating profile that is top-heavy, that of clouds-off is more symmetric about the middle troposphere (Figure 7b). Above the freezing level, the total heating in clouds-on is much larger (30–50%) than in clouds-off. This is mainly due to the large-scale heating, generated by microphysical processes acting on the grid-scale, that is important in determining the level where the heating maximizes (Figure 7d). Large-scale heating in the upper troposphere (between 400 and 300 hPa) strengthens considerably when cloud-radiative effects are active, and cooling is evident below the freezing level, indicative of more stratiform cloud processes. This leads to the total heating profile being more top-heavy. In contrast, the

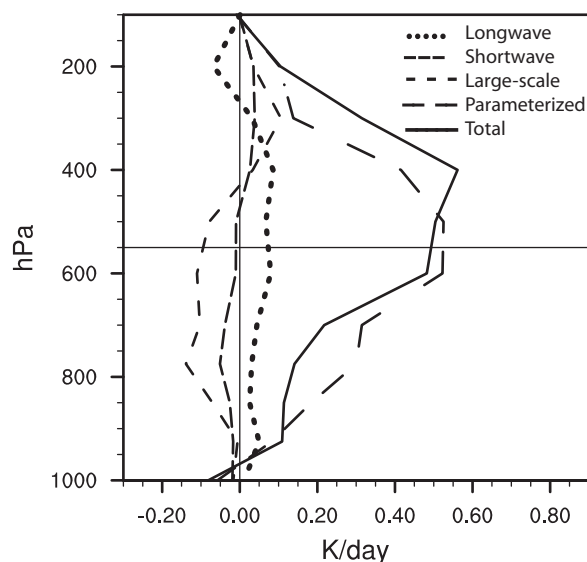


Figure 8. Heating rates composited to MJO deep convection over the Indian Ocean (averaged over 15°S–10°N, 60°E–90°E) in MPI-ESM clouds-on.

active phase of intraseasonal variability, cloud-radiative feedbacks lead to a strong modification of the heating profile with enhanced heating in clouds-on and a shift of the heating profile maximum from a mid-heavy to a top-heavy profile. This is mainly owing to the large-scale heating that modifies the parameterized heating profile, which otherwise dominates. *Li et al.* [2009] also found top-heavy profiles, but for standing intraseasonal waves, while for eastward propagating, MJO-like disturbances, bottom-heavy profiles occurred. To establish, whether this might also be the case for MPI-ESM clouds-on, we additionally performed profile composites based on the MJO index (see section 3.3). These composites represent the profiles during the MJO phase, when convection occurs over the Indian Ocean area (15°S–10°N and 60°E–90°E). The composite profiles (Figure 8) are similar to the regression-based profiles (Figure 7b) and demonstrates that in MPI-ESM not only intraseasonal variability in general, but especially the eastward propagating MJO is connected with a top-heavy profile under convective conditions. Similar profiles are found over the western Pacific under deep convective conditions (not shown).

4. Discussion

In this study, the contribution of cloud-radiative heating on the mean tropical climatology and its intraseasonal variability is investigated using four comprehensive atmosphere general circulation models. This investigation is facilitated through specially designed experiments in which clouds are made transparent to radiation (clouds-off). By performing the simulations with fixed sea-surface temperatures, this change primarily influences the atmospheric heating, and as such is dominated by longwave cloud-radiative effects. The COOKIE is not perfect, in that the land temperatures are allowed to respond to the changes in the radiation code, while the SSTs are not, which may generate land sea circulations that influence the interpretation of our results. Also, extratropical impacts via remote impacts, due to the fact that cloud cover is set to zero globally, cannot be excluded. To the extent these issues do not dominate, the simulations suggest that in all models investigated here, radiative heating by clouds has a strong influence on the mean state in the tropics. Making clouds transparent to radiation systematically alters the mean wind fields, in that it weakens the equatorial Indo-Pacific westerlies. Furthermore, the mean precipitation also changes, which is essentially manifested in a tendency to a double ITCZ. In the control (clouds-on) experiments, a single ITCZ is evident in the simulations by each of the models. When clouds are transparent to radiation, the ITCZ adopts a more double ITCZ structure. Thus, eliminating cloud-radiative interactions tends to modify the mean state in a way that it is more unrealistic and has been previously found to be related to a weaker MJO. And indeed, less of an MJO signal is apparent in each of the simulation pairs analyzed in this study, although the MJO is generally too weak also in the clouds-on simulations. This indicates that insufficient representations of

large-scale heating in clouds-off is substantially smaller than in clouds-on and has little effect on the total heating profile. The LW radiative heating profile also has a larger amplitude in the clouds-on as compared to the clouds-off simulation. In particular, around 200 hPa, we obtain a considerable LW cooling in clouds-on, which is plausible because of the very effective cooling of higher clouds (Figure 7e). This cooling further sharpens the total heating maximum in levels higher than 300 hPa in clouds-on. Below the freezing level, the total heating is similar for clouds-on and clouds-off. At these levels, the increased parameterized heating (Figure 7c) is roughly offset by enhanced large-scale cooling. The SW heating remains overall small and leads to negligible changes in response to cloud-radiative effects (not shown).

We conclude that during the convectively

cloud-radiative effects in GCMs could be a reason for both, unrealistic mean states and MJOs. Thus, it may be possible that enhancing cloud-radiative effects, or the link between convection and cloud-radiative heating, could enhance the MJO. This should be an issue of a future study.

A relationship between the ITCZ and MJO has also been inferred from observations [e.g., Yoneyama *et al.*, 2013; Wang and Magnusdottir, 2006; Lin *et al.*, 2006], however, predominantly for single MJO events, and with more of a focus on the position of the ITCZ rather than on changes that lead to a double or single ITCZ structure. Although we do not explain why cloud-radiative effects are important for the maintenance of a single ITCZ, ongoing work with the ECHAM model does suggest that in idealized aqua planet configurations the radiative effects of high clouds are crucial for maintaining a single ITCZ on the equator in the absence of a sufficiently strong equatorial SST maximum (B. Möbis, personal communication, 2015). Links between the ITCZ structure and the MJO are also evident in additional MPI-ESM AMIP experiments using a different convection scheme, and experiments performed with ECHAM5, the predecessor of ECHAM6 [Roeckner *et al.*, 2003]. In simulations using the original Tiedtke convection scheme, without the modifications introduced by Nordeng, a double ITCZ and a weak MJO are evident [Nordeng, 1994; Möbis and Stevens, 2012]. On the basis of the present results, we hypothesize that by making convection more sensitive to moisture in the lower-middle troposphere, the Nordeng scheme supports a stronger cloud-radiative feedback as compared to the Tiedtke scheme. This is supported by our moisture analysis that shows a stronger moisture sensitivity in middle and lower layers in MPI-ESM clouds-on than in clouds-off. As a consequence, both the Nordeng clouds-off and the Tiedtke AMIP experiment lead to a double ITCZ and a weak MJO. No consistent picture is obtained with respect to the response of the mean relationship between rain rates and relative humidity. Thus, a consistent impact of the moisture distribution onto the MJO has not been found across the models. But this may simply reflect differences in their parameterizations of convection and its sensitivity to humidity. MPI-ESM clouds-on precipitation rates reveal a slightly higher moisture sensitivity in the midlower troposphere (400–800 hPa) than clouds-off, accompanied by a stronger MJO than in clouds-off. Thus, for this model, the ideas of Kim *et al.* [2014b] are confirmed, who inferred that models producing a better MJO exhibit a larger contrast in lower tropospheric humidity between heavy and light rain events. In simulations by all of the four GCMs, atmospheric heating due to clouds strengthens eastward propagating MJO-like disturbances as compared to simulations where cloud-radiative effects are not present. This finding supports Bony and Emanuel [2005], who suggested that moist-radiative feedbacks destabilize propagating planetary scale disturbances with phase speeds near that observed for the present day MJO.

In the present study, it is also found that cloud-radiative effects act to slow the eastward propagation of the MJO. These findings support earlier results by Andersen and Kuang [2012] and Maloney [2009]. In both of these studies—using general circulation models with a super-parameterization and a Zhang and McFarlane convection scheme, respectively—the relationship between the MSE budget of intraseasonal disturbances was analyzed. Both studies suggest that the vertically integrated LW heating is a dominant source of MJO-MSE that maximizes on the westward flank of the MJO, thereby retarding its propagation, similar to what is found here (Figure 6). Support for our results is found in studies that investigate MSE budgets of observed MJOs. Inoue and Back [2015] investigated the TOGA COARE data and found a 5 day lag between MSE and radiative heating for periods larger than 20 days. Sobel *et al.* [2014] analyzed data of three active MJO events over the Indian Ocean, obtained during the DYNAMO fields campaign. They also found a lag between radiative forcing and MSE and generally emphasized the dominant role of radiative feedbacks with respect to the MJO MSE. In contrast, Kim *et al.* [2014a] found nearly no lag between MJO MSE and LW radiative forcing in their study utilizing Reanalysis and AVHRR OLR, however, they did not isolate the cloud-radiative effects.

A further finding of this study is that the total diabatic heating profile associated with intraseasonal convection in MPI-ESM clouds-on is top-heavy. This means, there is a pronounced maximum around 400 hPa, while the heating rate profile in the clouds-off is much weaker and has a broader and somewhat more midtropospheric maximum between 600 and 400 hPa. The most important contributor to this difference comes from the heating associated with microphysical processes operating on the grid-scale (e.g., the cloud, rather than the convection scheme, which is often interpreted as the stratiform or large-scale component of the convective heating). This reveals a dipole pattern in the MPI-ESM clouds-on experiment with a cooling in the lower and middle atmosphere and a warming above, which is nearly missing in the corresponding clouds-off experiment. Because it is manifest in the cloud scheme, it is consistent with the idea that cloud-radiative effects are important for this stratiform heating. Parameterized heating overall increases, when cloud-

radiative feedbacks are allowed, namely between 900 and 400 hPa. We believe that this additional heating is indirectly caused by the moister atmosphere (see Figure 3) in mid and lower levels, because entrainment leads to a weaker drying of the convective column as compared to clouds-off. Thus, convection and convective heating, respectively, is stronger in clouds-on than in clouds-off. In addition, reevaporation in the convective downdrafts is believed to be smaller in clouds-on, because of the moister surrounding air. Both effects lead to an enhancement of convective heating in clouds-on compared to clouds-off. On the other hand, the top-heavy profile implies an increase of gross moist stability, implying a stabilizing effect on the convective column. From this perspective, we hypothesize that deep convection is hampered at levels higher than about the freezing level, while the microphysics gets more important. Also, *Johnson and Ciesielski* [2000] argued that the top-heavy profile leads to the demise of convection in the course of the eastward propagation of the convectively active part of the MJO. Therefore, they inferred that upper tropospheric heating is crucial for the eastward propagation of a disturbance. This is consistent with our results that the eastward propagation is enhanced when upper tropospheric warming is present in the convectively active phase of the MJO. The importance of the large-scale heating in MPI-ESM in simulating a realistic MJO is also corroborated by former ECHAM versions, namely ECHAM4 and ECHAM5 [*Crueger et al.*, 2013]. Both revealed stronger eastward propagation strengths than MPI-ESM and larger large-scale rain proportions. Our results also confirm *Lin et al.* [2004] who argue that the vertical dipole stratiform heating is the dominant contributor to the top-heavy profile. They showed that models generally tend to reveal a too weak top-heaviness of the heating profile, and concluded that this bias could be a reason for the too weak MJO inherent for many GCMs.

Our study clearly demonstrated the importance of cloud-radiative feedbacks on the MJO, thereby revealing a relationship between the MJO, the mean state, the vertical heating profiles, and Kelvin waves. Still open is the question, whether the MJO responds directly to the radiation changes or indirectly to the changes of the mean state, and whether eventually enhanced cloud-radiation feedbacks would further strengthen the MJO. These questions will be topic of a future study.

Acknowledgments

This research has received funding from the European Union, Seventh Framework Program (FP7/2007–2013) under grant agreement 244067 and from the Cluster of Excellence “CliSA” (EXC177) of Hamburg funded through the German Science Foundations (DFG). We thank the modeling groups of Météo-France, the Meteorological Institute of Japan, and the Laboratoire de Météorologie Dynamique for running their simulations. The figures were performed using the NCAR Command Language (Version 6.2.1) [Software] (2014). Boulder, Colorado: UCAR/NCAR/CISL/VETS, <http://dx.doi.org/10.5065/D6WD3XH5>. The CMIP5/IPCC AR5, the MPI-ESM, and the “clouds-off” simulation data used in this study are available from the Earth System Grid Federation (<http://pcmdi9.llnl.gov/esgf-web-fe/>). The MPI-ESM data used for the heating rate analysis are stored on a local cluster and available on request. ERA-interim data sets are available from ECMWF (<http://apps.ecmwf.int/datasets/data/interim-full-daily/>). GPCP data sets are available from Global Energy and Water Exchanges Project (<http://www.gewex.org/gpcp.html>). We thank A. Sobel and an anonymous reviewer for their very helpful comments. Tobias Becker is thanked for carefully reading an earlier draft of this article.

References

- Andersen, J. A., and Z. Kuang (2012), Moist static energy budget of MJO-like disturbances in the atmosphere of a zonally symmetric aquaplanet, *J. Clim.*, 25(8), 2782–2804, doi:10.1175/JCLI-D-11-00168.1.
- Bony, S., and K. A. Emanuel (2005), On the role of moist processes in tropical intraseasonal variability: Cloud-radiation and moisture-convection feedbacks, *J. Atmos. Sci.*, 62(8), 2770–2789, doi:10.1175/JAS3506.1.
- Chikira, M. (2013), Eastward-propagating intraseasonal oscillation represented by Chikira-Sugiyama cumulus parameterization. Part II: Understanding moisture variation under weak temperature gradient balance, *J. Atmos. Sci.*, 71(2), 615–639, doi:10.1175/JAS-D-13-038.1.
- Crueger, T., B. Stevens, and R. Brokopf (2013), The Madden-Julian Oscillation in ECHAM6 and the introduction of an objective MJO metric, *J. Clim.*, 26(10), 3241–3257, doi:10.1175/JCLI-D-12-00413.1.
- Dee, D. P., et al. (2011), The ERA-interim Reanalysis: Configuration and performance of the data assimilation system, *Q. J. R. Meteorol. Soc.*, 137(656), 553–597, doi:10.1002/qj.828.
- Duchon, C. E. (1979), Lanczos filtering in one and two dimensions, *J. Appl. Meteorol.*, 18(8), 1016–1022.
- Dufresne, J.-L., et al. (2013), Climate change projections using the IPSL-CM5 earth system model: From CMIP3 to CMIP5, *Clim. Dyn.*, 40(9–10), 2123–2165, doi:10.1007/s00382-012-1636-1.
- Fermepin, S., and S. Bony (2014), Influence of low-cloud radiative effects on tropical circulation and precipitation, *J. Adv. Model. Earth Syst.*, 6, 513–526, doi:10.1002/2013MS000288.
- Gates, W. L. (1992), AMIP: The atmospheric model intercomparison project, *Bull. Am. Meteorol. Soc.*, 73(12), 1962–1970.
- Grabowski, W. W., and Moncrieff, M. W. (2004), Moisture-convection feedback in the tropics, *Q. J. R. Meteorol. Soc.*, 130, 3081–3104.
- Houze, R. A. (1982), Cloud clusters and large-scale vertical motions in the tropics, *J. Meteorol. Soc. Jpn.*, 60(1), 396–410.
- Huffman, G. J., R. F. Adler, M. M. Morrissey, D. T. Bolvin, S. Curtis, R. Joyce, B. McGavock, and J. Susskind (2001), Global precipitation at one-degree daily resolution from multisatellite observations, *J. Hydrometeorol.*, 2(1), 36–50.
- Inoue, K., and L. E. Back (2015), Column-integrated moist static energy budget analysis on various time scales during TOGA COARE, *J. Atmos. Sci.*, 72, 1856–1871.
- Johnson, R. H., and Ciesielski, P. E. (2000), Rainfall and radiative heating rates from TOGA COARE atmospheric budgets, *J. Atmos. Sci.*, 57, 1497–1514.
- Kiladis, G. N., M. C. Wheeler, P. T. Haertel, K. H. Straub, and P. E. Roundy (2009), Convectively coupled equatorial waves, *Rev. Geophys.*, 47(2), RG2003, doi:10.1029/2008RG000266.
- Kim, D., A. H. Sobel, E. D. Maloney, D. M. W. Frierson, and I.-S. Kang (2011a), A systematic relationship between intraseasonal variability and mean state bias in AGCM simulations, *J. Clim.*, 24(21), 5506–5520, doi:10.1175/2011JCLI4177.1.
- Kim, D., A. H. Sobel, and I.-S. Kang (2011b), A mechanism denial study on the Madden-Julian Oscillation, *J. Adv. Model. Earth Syst.*, 3, M12007, doi:10.1029/2011MS000081.
- Kim, D., J.-S. Kug, and A. H. Sobel (2014a), Propagating versus nonpropagating Madden-Julian Oscillation events, *J. Clim.*, 27, 111–125, doi:10.1175/JCLI-D-13-00084.1.
- Kim, D., et al. (2014b) Process-oriented MJO simulation diagnostic: Moisture sensitivity of simulated convection, *J. Clim.*, 27(14), 5379–5395, doi:10.1175/JCLI-D-13-00497.1.
- Lappen, C.-L., and C. Schumacher (2012), Heating in the tropical atmosphere: What level of detail is critical for accurate MJO simulations in GCMs?, *Clim. Dyn.*, 39(9–10), 2547–2568, doi:10.1007/s00382-012-1327-y.

- Lau, K. M., H. T. Wu, Y. C. Sud, and G. K. Walker (2005), Effects of cloud microphysics on tropical atmospheric hydrologic processes and intraseasonal variability, *J. Clim.*, *18*(22), 4731–4751, doi:10.1175/JCLI3561.1.
- Lee, M.-I., I.-S. Kang, J.-K. Kim, and B. E. Mapes (2001), Influence of cloud-radiation interaction on simulating tropical intraseasonal oscillation with an atmospheric general circulation model, *J. Geophys. Res.*, *106*(D13), 14,219–14,233, doi:10.1029/2001JD900143.
- Li, Y., X. Jia, J. Ling, W. Zhou, and C. Zhang (2009), Sensitivity of MJO simulations to diabatic heating profiles, *Clim. Dyn.*, *32*(2–3), 167–187, doi:10.1007/s00382-008-0455-x.
- Lin, J., B. Mapes, M. Zhang, and M. Newman (2004), Stratiform precipitation, vertical heating profiles, and the Madden-Julian Oscillation, *J. Atmos. Sci.*, *61*(3), 296–309.
- Lin, J.-L., et al. (2006), Tropical intraseasonal variability in 14 IPCC AR4 climate models. Part I: Convective signals, *J. Clim.*, *19*(12), 2665–2690, doi:10.1175/JCLI3735.1.
- Lin, J.-L., D. Kim, M.-I. Lee, and I.-S. Kang (2007), Effects of cloud-radiative heating on atmospheric general circulation model (AGCM) simulations of convectively coupled equatorial waves, *J. Geophys. Res.*, *112*, D24107, doi:10.1029/2006JD008291.
- Maloney, E. D. (2009), The moist static energy budget of a composite tropical intraseasonal oscillation in a climate model, *J. Clim.*, *22*(3), 711–729, doi:10.1175/2008JCLI2542.1.
- Mehta, A. V., and E. A. Smith (1997), Variability of radiative cooling during the Asian summer monsoon and its influence on intraseasonal waves, *J. Atmos. Sci.*, *54*(8), 941–966.
- Möbis, B., and B. Stevens (2012), Factors controlling the position of the intertropical convergence zone on an aquaplanet, *J. Adv. Model. Earth Syst.*, *4*, M00A04, doi:10.1029/2012MS000199.
- Neelin, J. D., and I. M. Held (1987), Modeling tropical convergence based on the moist static energy budget, *Mon. Weather Rev.*, *115*(1), 3–12.
- Nordeng, T. (1994), Extended versions of the convective parameterization scheme at ECMWF and their impact on the mean and transient activity of the model in the tropics, *Tech. Memo. 206*, 41 pp., Eur. Cent. for Medium Range Weather Forecasts, Reading, U. K.
- Roeckner, E., et al. (2003), The atmospheric general circulation model ECHAM5—Part I: Model description, *Tech. Rep. 349*, Max-Planck-Inst. für Meteorol., Hamburg, Germany.
- Slingo, J. M., et al. (1996), Intraseasonal oscillations in 15 atmospheric general circulation models: Results from an AMIP diagnostic subproject, *Clim. Dyn.*, *12*(5), 325–357, doi:10.1007/BF00231106.
- Sobel, A., and E. Maloney (2013), Moisture modes and the eastward propagation of the MJO, *J. Atmos. Sci.*, *70*(1), 187–192, doi:10.1175/JAS-D-12-0189.1.
- Sobel, A., S. Wang, and D. Kim (2014), Moist static energy budget of the MJO during DYNAMO, *J. Atmos. Sci.*, *71*(11), 4276–4291.
- Sperber, K. R., S. Gualdi, S. Legutke, and V. Gayler (2005), The Madden-Julian Oscillation in ECHAM4 coupled and uncoupled general circulation models, *Clim. Dyn.*, *25*(2–3), 117–140, doi:10.1007/s00382-005-0026-3.
- Stevens, B., M. Bony, and M. Webb (2012), Clouds on-off climate intercomparison experiment (COOKIE). [Available at <http://www.euclipse.eu/wp4/wp4.html>.]
- Stevens, B., et al. (2013), Atmospheric component of the MPI-M earth system model: ECHAM6, *J. Adv. Model. Earth Syst.*, *5*, 146–172, doi:10.1002/jame.20015. [10.1002/jame.20015].
- Taylor, K. E., R. J. Stouffer, and G. A. Meehl (2012), An overview of CMIP5 and the experiment design, *Bull. Am. Meteorol. Soc.*, *93*(4), 485–498, doi:10.1175/BAMS-D-11-00094.1.
- Thayer-Calder, K., and D. A. Randall (2009), The role of convective moistening in the Madden-Julian Oscillation, *J. Atmos. Sci.*, *66*, 3297–3312.
- Volz, A., et al. (2013), The CNRM-CM5.1 global climate model: Description and basic evaluation, *Clim. Dyn.*, *40*(9–10), 2091–2121, doi:10.1007/s00382-011-1259-y.
- von Storch, H., and F. Zwiers (1999), *Statistical Analysis in Climate Research*, 494 pp., Cambridge Univ. Press, Cambridge, U. K.
- Waliser, D., et al. (2009), MJO simulation diagnostics, *J. Clim.*, *22*(11), 3006–3030, doi:10.1175/2008JCLI2731.1.
- Wang, C.-C., and G. Magnusdottir (2006), The ITCZ in the central and eastern Pacific on synoptic time scales, *Mon. Weather Rev.*, *134*(5), 1405–1421, doi:10.1175/MWR3130.1.
- Wheeler, M. C., and H. H. Hendon (2004), An all-season real-time multivariate MJO index: Development of an index for monitoring and prediction, *Mon. Weather Rev.*, *132*(8), 1917–1932.
- Yoneyama, K., C. Zhang, and C. N. Long (2013), Tracking pulses of the Madden-Julian Oscillation, *Bull. Am. Meteorol. Soc.*, *94*(12), 1871–1891, doi:10.1175/BAMS-D-12-00157.1.
- Yukimoto, S., et al. (2012), A new global climate model of the meteorological research institute: MRI-CGCM3—Model description and basic performance, *J. Meteorol. Soc. Jpn.*, *90A*, 23–64, doi:10.2151/jmsj.2012-A02.
- Zhang, C., M. Dong, S. Gualdi, H. H. Hendon, E. D. Maloney, A. Marshall, K. R. Sperber, and W. Wang (2006), Simulations of the Madden-Julian Oscillation in four pairs of coupled and uncoupled global models, *Clim. Dyn.*, *27*(6), 573–592, doi:10.1007/s00382-006-0148-2.